

Adsorption kinetic, equilibrium and thermodynamic studies for the removal of Acid Blue-25 from aqueous solution by using ecofriendly stishovite clay and its nanocomposite with MnO_2 – A comparative study

K. Prabhakaran¹, T. Mohanapriya²

¹*Center for Environmental Research, Department of Chemistry, Kongu Engineering College, Perundurai, Erode, Tamil Nadu, India.*

²*Department of Chemistry, Erode Arts and Science College, Erode, Tamil Nadu, India*

Abstract- Artificial dye pollution in the water sector has major negative effects on human health and raises environmental issues. Various sectors, such as paper and textiles, release dyes into water bodies, causing significant ecological imbalances and endangering human health. This work aims to investigate the viability of employing the Stishovite- MnO_2 nanocomposite as an adsorbent to remove acid blue 25 (AB-25). Alcohol is then added to commercially available Stishovite clay and MnO_2 , which are then dried and put to use. Numerous operating parameters, including initial dye concentration, contact time, adsorbent dose, pH, and temperatures, have been used in batch adsorption investigations. The Langmuir, Freundlich, Tempkin, and Halsey isotherms all fit the equilibrium data quite well. These are used to determine the dimensionless separation factor, adsorption energy, adsorption capacity, adsorption intensity, and adsorption efficiency. The Elcovich model and pseudo second order kinetic model both suit the experiment results quite well, indicating chemisorptions that are supported by desorption studies.

Keywords: Dye removal, Nanocomposite, adsorption isotherm, kinetics, desorption.

1. INTRODUCTION

Due to their high toxicity and colour strength, dyes that are continuously released from the industries that manufacture and consume them have recently caused a significant deal of public worry. The current century's massive industrial numbers have been shown [1]. Because water supplies are limited, water contamination is one of the most significant environmental problems that the globe faces. More than 700,000–1000,000 colours are thought to be

created annually by various industrial processes, including those in the food processing, textile, paper, rubber, plastics, cosmetics, and pharmaceutical industries [2]. Although cationic dyes are frequently used in the industry, they are more dangerous than other types. An estimated 12% of the annual output of cationic dyes is wasted in industrial water streams, which affects the environment [3]. The majority of these colours exhibit teratogenicity, skin irritation, carcinogenicity, toxicity, non-biodegradability, and impacts on mutations and allergic dermatitis. Moreover, it poses major risks to ecosystems and human health [4,5]. As a result, several effective methods were investigated to remove these contaminants from wastewater. The most common methods include chemical oxidation, electrochemical treatment, coagulation, biological degradation, ozonation, nanofiltration, reverse osmosis, advanced oxidation processes, and photocatalytic degradation, which includes aerobic and adsorption [6–8]. These days, a lot of adsorbent materials made from agricultural waste are used to remove colours from wastewater. These materials have several benefits over more conventional materials, including being economical, effective, biodegradable, and renewable [9]. Therefore, some examples of these prospective adsorbent materials are carboxymethyl cellulose (CMC) [11], pinewood [12], wheat [13], and biochar (rice husk) [14], which are all effective adsorbents. Clay materials are among the most unusual adsorbent materials; they are widely used and come in a lot of different forms. Furthermore, clay materials decompose naturally [15,16].

The goal of the current study was to determine whether stishovite clay and its nanocomposite could be used to adsorb Acid Blue-25 from aqueous solution. The purpose of the batch adsorption tests was to compare the adsorbents' adsorption efficiency. Langmuir and Freundlich adsorption isotherms were used to describe the adsorption process, and the values of the parameters associated with these isotherms were assessed. Using raw stishovite clay and its nanocomposites, the thermodynamic parameters—Gibbs free energy change (ΔG), enthalpy change (ΔH), and entropy change (ΔS)—were calculated for the Acid blue-25 adsorption in order to estimate the mechanism, nature, feasibility, and spontaneity of the adsorption process.

2. MATERIALS AND METHODS

In order to verify the creation of a superior, eco-friendly nanocomposite with effective dye removal capabilities, the components used in this work were carefully selected. Manganese dioxide (MnO_2) and Stishovite clay nanoparticles are acquired from TEQTO Scientific Company in Coimbatore, India. Both substances serve as essential components. Stishovite clay was chosen because of its unique crystalline structure and remarkable surface area, which make it an excellent adsorption foundation material. The incorporation of MnO_2 nanoparticles was motivated by their intrinsic catalytic and adsorptive characteristics. To achieve the appropriate dispersion of the MnO_2 nanoparticles inside the clay matrix, ethanol was employed as a solvent during the synthesis procedure. Ethanol's low toxicity and facile elimination made it an appropriate option for this environmentally friendly synthesis technique. Purification and washing procedures were carried out using double-distilled water to guarantee the absence of impurities in all components and synthesised composites. Using double-distilled water guaranteed the nanocomposite's greatest degree of purity, which was critical for exact characterisation and consistent performance in subsequent dye removal experiments. A stock solution (1000mg/L) of dye was made using doubly distilled water. Diluting the stock dye solution yields a variety of dye solutions with varying starting concentrations. The adsorbate employed in this investigation is Acid Blue-25 (AB-25). Using double-distilled water guaranteed the nanocomposite's

greatest degree of purity, which was critical for exact characterisation and consistent performance in subsequent dye removal experiments. A stock solution (1000mg/L) of dye was made using doubly distilled water. Diluting the stock dye solution yields a variety of dye solutions with varying starting concentrations. The adsorbate employed in this investigation is Acid Blue-25 (AB-25).

2.1 CHARACTERIZATION OF ADSORBENT

The crystallographic phase of stishovite clay and stishoviteclay- MnO_2 nanocomposites was determined by X-ray diffraction (XRD) research. The XRD pattern of stishovite clay shows distinct peaks, indicating a tetragonal crystal structure. The presence of these distinct peaks confirms the integrity and crystalline structure of the stishovite clay, which is free of any apparent impurities or non-crystalline phases. Adding MnO_2 nanoparticles to the stishovite clay matrix resulted in significant changes to the nanocomposite's XRD pattern. The nanocomposite showed the characteristic stishovite peaks, but with reduced intensity and progressive widening, indicating a partial disruption of the crystal lattice due by the addition of MnO_2 . The XRD pattern revealed several additional peaks associated with MnO_2 , confirming its successful amalgamation into the clay matrix. MnO_2 -related peaks were less intense compared to those of stishovite. This is due to the composite's decreased MnO_2 content and fine particle dispersion within the clay matrix. The expansion of these peaks shows the existence of MnO_2 nanoparticles with tiny crystallite diameters, which are typical of nanocomposites and helpful for enhancing the adsorption surface area.

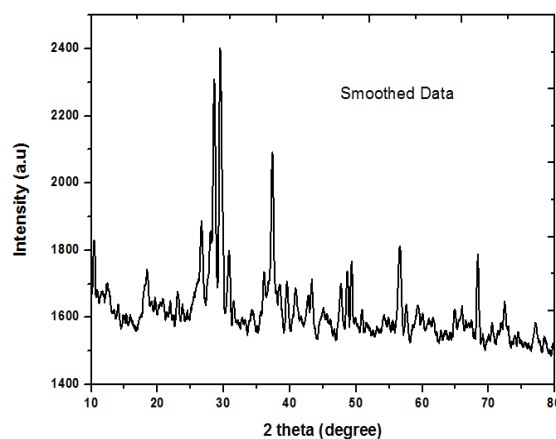


Figure 1(a) XRD Analysis of stishovite clay

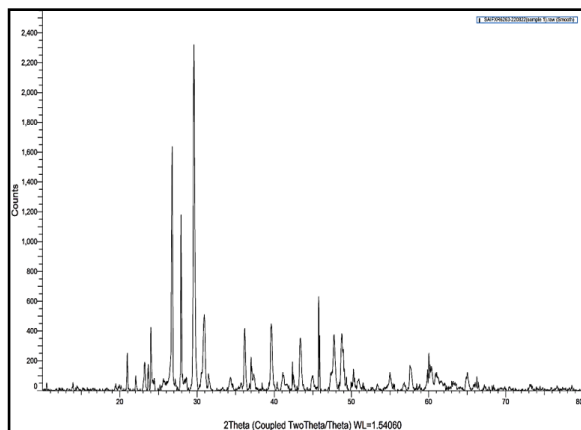


Figure 1(b) XRD Analysis of stishovite clay - MnO_2 nanocomposite

Figures 2(a) and 2(b) show SEM images of samples containing stishovite clay and stishovite clay- MnO_2 nanocomposite, respectively. Surface changes detected in the stishovite clay- MnO_2 nanocomposite vs stishovite clay. Stishovite clay was made up of irregularly sized and shaped flakes with damaged borders [45]. This clay has the capacity to stick to and stab into one another. This structure was compact and dense, indicating that the particles were highly crystalline. This is typical of natural clay materials, since the surface seemed smooth with some little porosity.

Adding MnO_2 nanoparticles increased surface roughness and heterogeneity. MnO_2 nanoparticles were found in small, homogeneous amounts on the surface of stishovite clay particles. These nanoparticles led to a porous and uneven surface, which is beneficial for increasing the composite's adsorption capacity. The creation of nanostructures indicates an increase in surface area, as does a modification in surface shape. This increase is critical for improving the composite's adsorptive characteristics. The SEM investigation confirmed the effective integration of MnO_2 into the stishovite clay matrix, with no obvious signs of aggregation, indicating the nanoparticles were well disseminated.

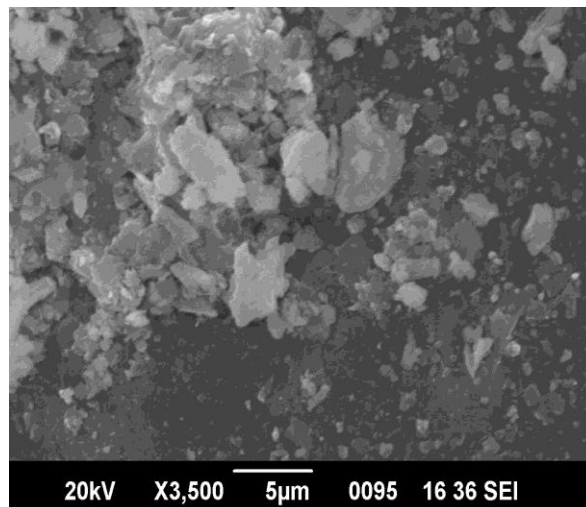


Figure 2 (a) SEM of stishovite clay

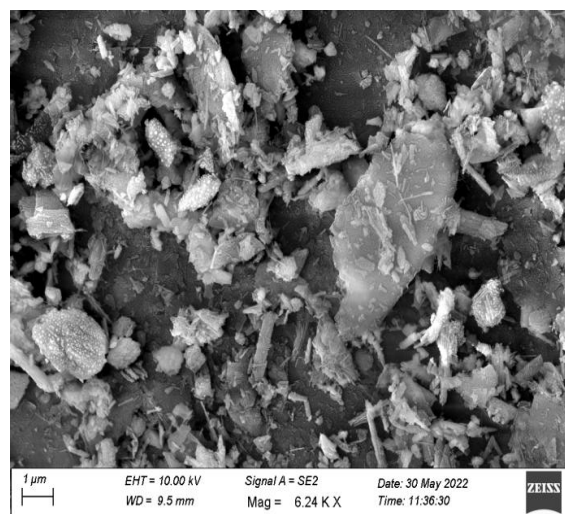


Figure 2 (b) SEM of stishovite clay - MnO_2 nanocomposite

FTIR SPECTROSCOPY

The adsorption band in stishovite clay, located between 3580 and 3690 cm^{-1} , is caused by the -OH stretching vibration of the water molecule. This band moved to 3710 cm^{-1} in the stishovite clay- MnO_2 nanocomposite. The twisting motion of the H-O-H group of water molecules adsorbed on the nanocomposite structure was discovered to be associated with the band at 1665 cm^{-1} . Spectral peaks at 513.81 cm^{-1} are attributed to the O-Mn-O and Mn-O vibrations. The bending vibrations of the Si-O-Al and Si-O-Si clusters were measured at around 518.81 cm^{-1} . The addition of MnO_2 nanoparticles conserved

the Si-O-Si structure of stishovite clay, as shown by the FT-IR spectra of the stishovite-MnO₂ nanocomposite, which had similar absorption bands. The nanocomposite spectra revealed additional absorption bands at 558.48 cm⁻¹, indicating Mn-O vibrations and verifying the presence of MnO₂ in the composite. The FT-IR analysis verified the existence of both stishovite clay and MnO₂ inside the nanocomposite, with little degradation of the clay's structure and good MnO₂ integration.

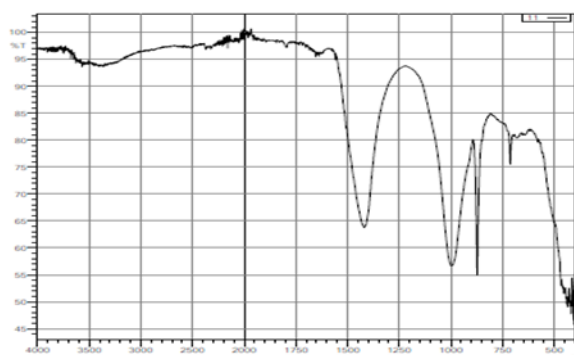


Figure 3(a) FT-IR spectra for stishovite clay

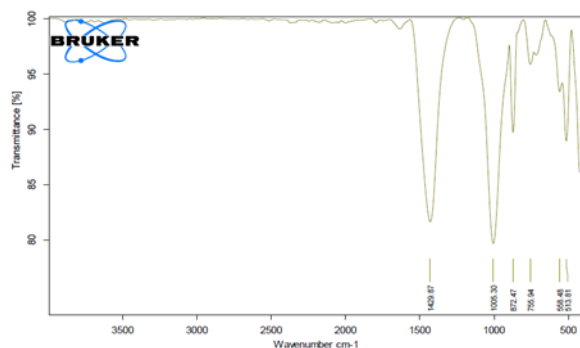


Figure 3(b) FT-IR spectra for stishovite clay - MnO₂ nanocomposite

III. BATCH ADSORPTION EXPERIMENTS

Entire batch mode tests were performed in the temperature range of 303K to 311K, using 50ml of the corresponding dye solution and a specified quantity of adsorbent in a 100ml conical flask. The flasks were stirred at certain time intervals in a thermostat connected to a shaker at the desired temperature. The adsorbent and adsorbate were separated via filtering. The effects of agitation duration, pH, beginning concentration, adsorbent dosage, and temperature

were investigated using a known quantity of adsorbent and 50ml of dye solution at various concentrations. A dye solution (50ml) containing varying concentrations of adsorbent was used to investigate the effect of adsorbent dose on dye removal.

3.1 EFFECT OF AGITATION TIME AND INITIAL DYE CONCENTRATION

The effect of initial dye concentration and contact time for the removal of AB-25 in stishovite clay and stishovite clay- MnO₂ nanocomposite is shown in Fig.4(a) and 4(b). For this study 50ml of 10 to 40mg/L of dye solution was agitated with 100mg of adsorbent. The extent of removal of dye was faster in initial stages, then showed decreasing pattern and finally became constant showing the attainment of equilibrium. The extent of removal was found in stishovite clay to be 74% and the removal was found in stishovite clay-MnO₂ nanocomposite to be 90.53%.

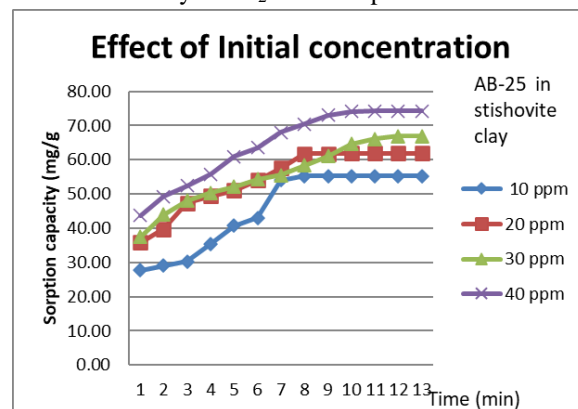


Fig.4(a)

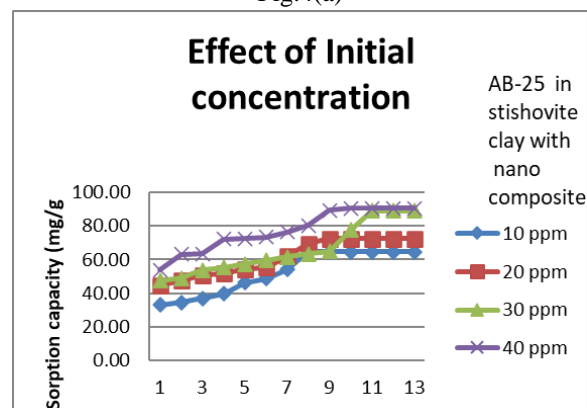


Fig.4(b)

3.2 EFFECT OF ADSORBENT DOSAGE ON ADSORPTION PROCESS

The impact of adsorbent dose on acid dye removal was investigated while maintaining all other experimental

conditions constant except the adsorption dosage. The quantity adsorbed per unit mass of the adsorbent decreased as the adsorbent concentration increased (Figs. 5(a) and 5(b)). The reduction in unit adsorption with increased adsorbent dose may be attributed to the fact that adsorption sites remain unsaturated during the adsorption process.

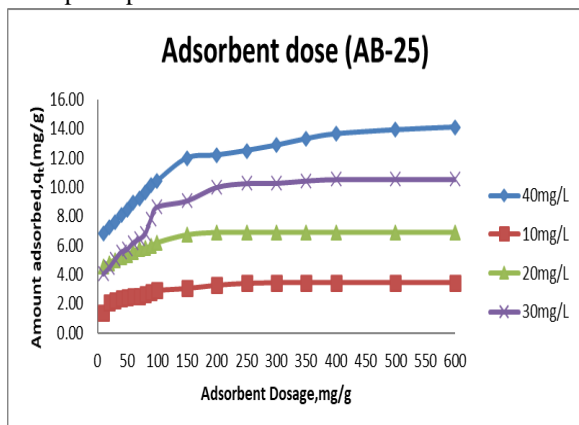


Fig.5(a)

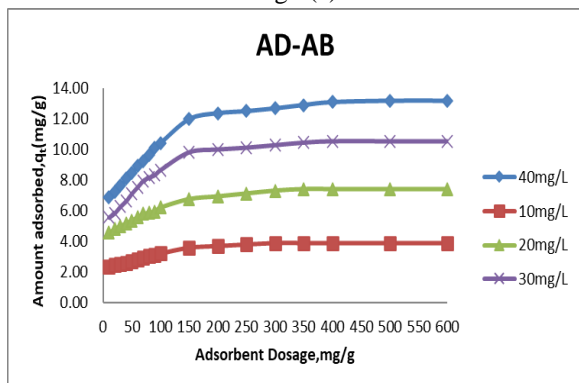


Fig.5(b)

3.3 EFFECT OF pH

Adsorption studies were performed at pH values ranging from 6 to 11 while maintaining the requisite pH by adding the appropriate amount of dilute hydrochloric acid and sodium hydroxide solutions. A pH meter calibrated with 4.0 and 9.0 buffers was utilised. Figures 6(a) and 6(b) show that greatest dye removal occurred in an acidic medium. It was found that when the pH increased, so did the sorption capacity. The pH zpc values for the stishovite clay and stishovite clay MnO₂ nanocomposite were 6.0 and 6.5, respectively.

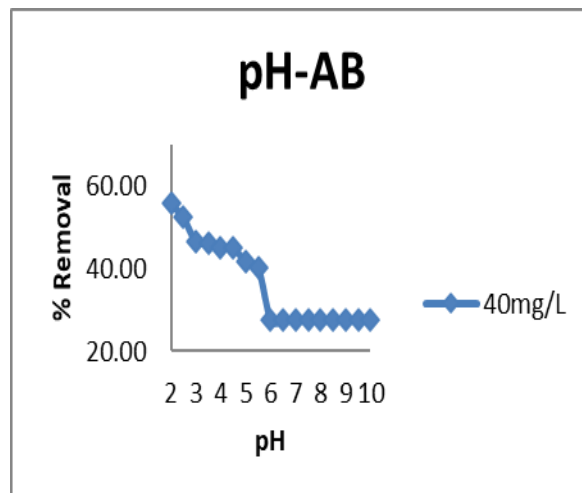


Fig. 6(a)

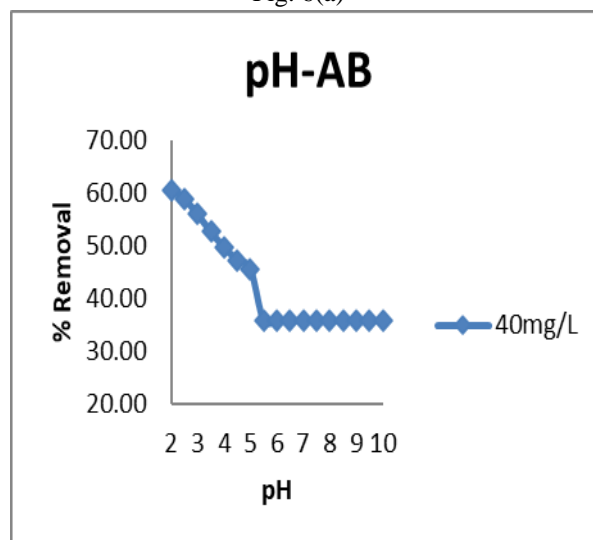


Fig. 6(B)

3.4 EFFECT OF TEMPERATURE

Temperature has a significant impact on the sorption process. Figures 7(a) and 7(b) demonstrate the effect of different temperatures on AB-25 removal by clay and nanocomposites. The quantity of acid dye adsorbed rises with increasing temperature, from 303K to 311K, demonstrating that the adsorption process is endothermic. This might be because when the temperature rises, the rate of diffusion of adsorbate molecules across the exterior boundary layer and interior pores of the adsorbent particle increases.

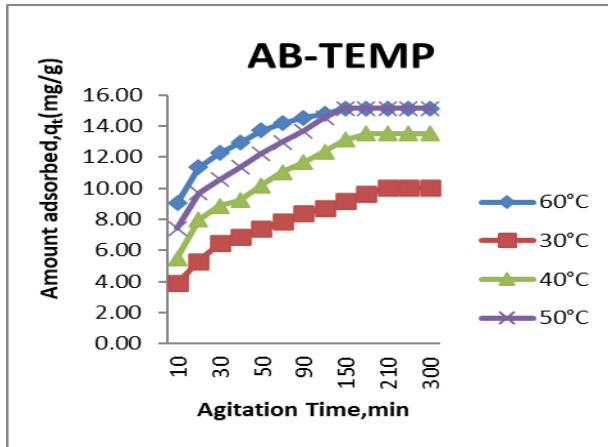


Fig. 7(a)

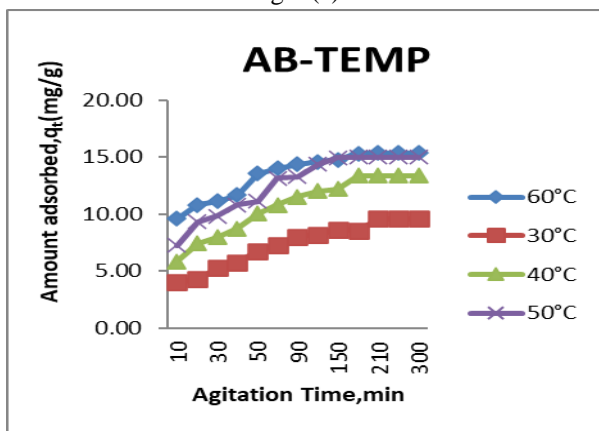


Fig. 7(b)

3.5 ADSORPTION ISOTHERM

The link between the amount of dye adsorbed and its equilibrium concentration was investigated using Langmuir and Freundlich isotherms.

3.5.1 Langmuir isotherm

The Langmuir adsorption isotherm, which implies that adsorption occurs at particular homogenous locations inside the adsorbent, has been effectively applied to various situations involving monolayer adsorptions.

$$C_e/q_e = 1/bq_0 + C_e/q_0 \quad (1)$$

Where C_e is the adsorbate's equilibrium concentration (mg/L), q_e is the amount of dye adsorbed per unit mass adsorbent (mg/L), and q_0 and b are Langmuir constants for adsorption capacity and rate, respectively. As indicated by equation (1), graphing C_e/q_e vs C_e yielded a straight line, demonstrating that acid dye adsorption on the nanocomposite follows the

Langmuir isotherm. The Langmuir constants b and q_0 were calculated using the slope and intercept of the graph.

The essential characteristics of the Langmuir isotherm can be expressed in terms of a dimensionless equilibrium parameter R_L which is represented by,

$$R_L = 1/(1 + b C_0) \quad (2)$$

Where, C_0 is the highest initial solute concentration, 'b' the Langmuir adsorption constant (L/mg).

If the value of R_L is less than one then it indicates favorable adsorption. The R_L values shown in Table 1 all are less than indicating the applicability of Langmuir isotherm to this adsorption process.

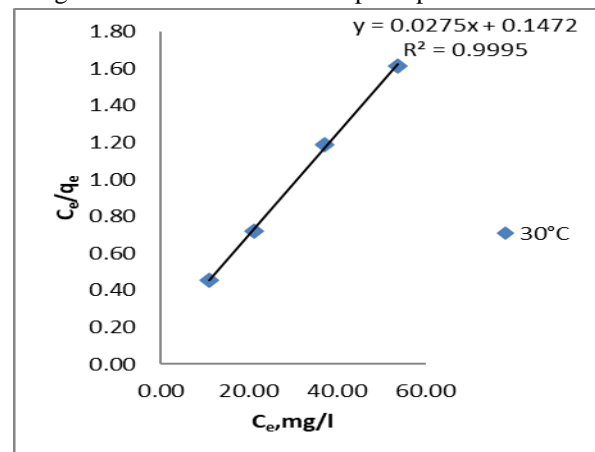


Fig. 8(a)

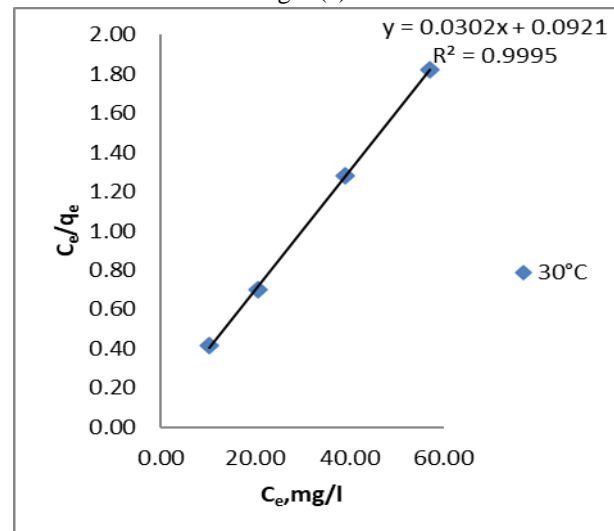


Fig. 8(b)

Table 1. The values of Langmuir constant Q^0 and b in addition to R_L

Concentration of dye (mg/L)	Acid blue 25 in stishovite clay			
	R _L	B	Q ⁰ mg/g	R ²
20	0.9916			
40	0.9845			
60	0.9865	0.000301	49.765	0.9912
80	0.9743			
100	0.9716			
120	0.9655			

Concentration of dye (mg/L)	Acid blue 25 in stishovite clay with MnO ₂ nanocomposite			
	R _L	B	Q ⁰ mg/g	R ²
20	0.9929			
40	0.9878			
60	0.9829	0.000315	58.128	0.9964
80	0.9754			
100	0.9713			
120	0.9644			

3.5.2 Freundliche Model

The Freundlich isotherm, an empirical connection used to explain heterogeneous systems, may be stated in its logarithmic form (Eq. 3).

$$\log q_e = \log K_f + 1/n \log C_e \quad (3)$$

Where K_f and $1/n$ are Freundlich constants representing the sorbent's adsorption capacity and intensity, respectively. q_e is the quantity adsorbed at equilibrium (mg/g), and C_e is the adsorbate's equilibrium concentration. Tables 3 and 4 show the computed values of K_f and $1/n$ based on the intercept and slope. The plot of $\log q_e$ vs $\log C_e$ yielded a straight line (Fig. 9(a) and 9(b) with an excellent regression coefficient, demonstrating that AB-25 adsorption follows the Freundlich isotherm.

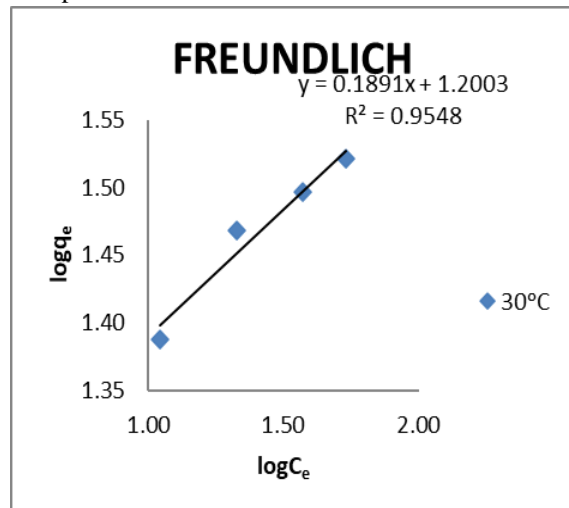


Fig. 9(a) –Stishovite clay

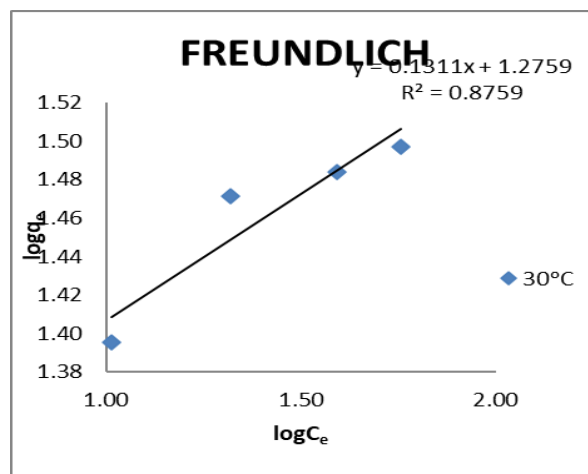


Fig. 9(b) –Stishovite clay with MnO₂ nanocomposite.

3.6 Kinetics of adsorption

In order to investigate the mechanism of adsorption of Acid blue -25 by the stishovite clay and stishovite clay with MnO₂ nanocomposite the following three kinetic models were considered.

3.6.1 Pseudo first order kinetic model

The integrated linear form of this model proposed by Lagergren (Eq.4):

$$\log (q_e - q_t) = \log q_e - (k_1/2.303) t \quad (4)$$

Where q_e is the amount of dye adsorbed at equilibrium (mg/g), and q_t is the amount of dye adsorbed (mg/g) at time t , k_1 is the first order rate constant (min^{-1}) and t is time (min). Hence a linear trace expected between the two parameters $\log (q_e - q_t)$ and t , provided the adsorption follows first order kinetics. It is observed that the data does not fit in to first order equation.

3.6.2 Pseudo second order kinetics

The adsorption may also be described by pseudo second order kinetic model. The linearized form of the pseudo order model (Eq.5):

$$t/q_t = 1/k_2 q_e^2 + 1/q_e * t \quad (5)$$

where k_2 is the second order rate constant (g/mg min). A plot of t/q_t vs t should be linear if the adsorption follows second order. q_e and k_2 can be calculated from the slope and intercept of the plot. AB-25 obeys the pseudo order kinetics.

3.7. Elovich kinetic model

The Elovich equation is mainly applicable for chemisorptions processes involving heterogeneous adsorbing surfaces. The Elovich model in its integrated form can be

$$Q_t = (1/b) \ln(ab) + (1/b) \ln t \quad (6)$$

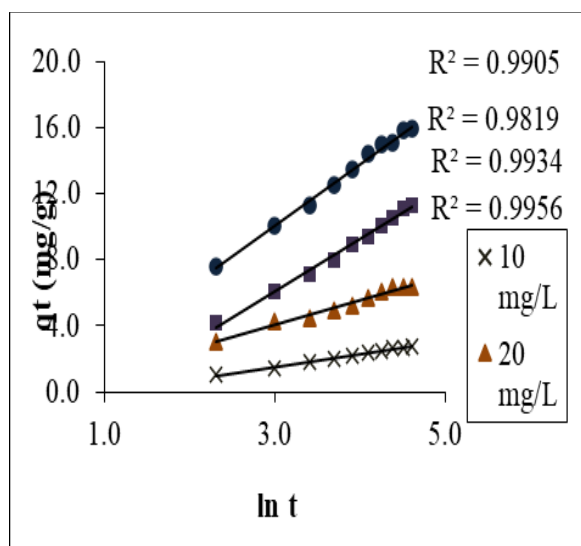


Fig. 10: Elkovich kinetic model

Where 'a' is the initial adsorption rate (mg/g min) and 'b' is related to the extent of coverage and the activation energy for chemisorptions (g/mg). A plot of q_t vs $\ln t$ is a straight line, as expected, which a slope of $1/b$ and an intercept $\log 1/b \ln(ab)$ with good correlation coefficients conforming the chemisorptive nature of adsorption.

3.8 Thermodynamic of Adsorption

Thermodynamic parameters like ΔH° and ΔS° were evaluated using Van't Hoff equation:

$$\ln K_c = \Delta S^\circ / R - \Delta H^\circ / RT \quad (8)$$

Where K_c is the Langmuir equilibrium constant, ΔH° and ΔS° are the standard enthalpy and entropy changes of adsorption respectively and their values are calculated from the slopes and intercepts respectively of the linear plot of $\ln K_c$ vs $1/T$. The free energy change for the adsorption process ΔG° (kJ/mol) is derived (Eq.9):

$$\Delta G^\circ = \Delta H^\circ - T \Delta S^\circ \quad (9)$$

Negative free energy change and positive endropy change of adsorption (Table 3) indicate that the adsorption process is favorable and spontaneous in nature. The endothermic nature of adsorption is confirmed by the positive ΔH° value.

Table 3: Thermodynamic parameters for adsorption of AB-25 on Stichovite –MnO₂ Nanocomposite.

DYES	- ΔG° (kJ/mol)			ΔS° (kJ/mol)	ΔH° (kJ/mol)
	303K	307K	311K		
AB-25	1.732	1.744	1.753	5.435	20.001

IV. DESORPTION INVESTIGATIONS.

Desorption tests with acetic acid revealed that adsorbent regeneration was ineffective, confirming the chemisorptive nature of adsorption.

V. CONCLUSION

The current study shown that stishovite clay and stishovite clay-MnO₂ nanocomposite may be employed as adsorbents for the elimination of acid blue (AB-25). The amount of dye adsorbed varied according to starting dye concentration, adsorbent dosage, pH, and temperature. The removal of acid blue by clay and nanocomposite followed both the Langmuir and Freundlich isotherms. The adsorption process followed pseudo-second order kinetics. This is supported by the Elkovich chemisorptive kinetic model. Desorption experiments reveal that no adequate results occur in accordance with the chemisorptive nature of adsorption. The evaluation of thermodynamic parameters revealed that the process was endothermic and spontaneous.

REFERENCES

- [1] Adeanmi, B.M., Hung, Y.T., Paul, H.H and Huhnke, C.R., Comparison of dye wastewater treatment methods: A review, GSC Adv. RES. REV., 10(2), 126-137 (2022).
- [2] Noreen S, Tahira M, Ghamkhar M, Hafiz I, Bhatti HN, Nadeem R, et al. Treatment of textile wastewater containing acid dye using novel polymeric grapheme oxide nanocomposites (GO/PAN, GO/PPy, GO/PSty). Mater Re Technol 2021;14:25-35. <https://doi.org/10.1016/j.mrt.2021.06.007>
- [3] Foroutan R, Mohammadi R, Sohrabi N, sehebi S, Farjdfard S, Esvandi Z, Ramavandi B. Calcined alluvium of agricultural streams as a recyclable and cleaning tool for cationic dye removal from aqueous media. Environ Tecnol Innovat 2020;17:100530. <https://doi.org/j.eti.2019.100530>.
- [4] Grassi P, Drumm FC, pannenberg SS, Georgin J, Tonato D, Mazutti MA, et al. Solid wastes from enzyme production as a potential biosorbent to treat colored effluents containing crystal violet dye. Environ Sci Pollute Res 2020;27:10484-94. <http://doi.org/10.1007/s11356-020-07664-0>.

- [5] Liu L, Gao ZY, Su XP, Chen X, Jiang L, Yao JM. Adsorption removal of dyes from single and binary solutions using a cellulose-based bioadsorbent. *ACS sustainable Chem Eng* 2015;3:432-42.
<https://doi.org/10.1021/sc500848m>.
- [6] Wang RF, Deng LG, Li K, Fan XJ, Li W, Lu HQ. Fabrication and characterization of sugarcane bagasse-calcium carbonate composite for the efficient removal of crystal violet dye from wastewater. *Cream Int* 2020;46:27484-92.
<https://doi.org/10.1016/j.ceramint.2020.07.237>.
- [7] Yuan L, Jiang W. Porous cellulose triacetate particles prepared from recycled corrugated cases for adsorption of crystal violet. *Jappl Polym Sci* 2021;138:50981.
<https://doi.org/10.1002/app.50981>.
- [8] Khan MM, Khan Amina, Bhatti HN, Zahid M, Alissa SA, El-Badry YA, et al. Composite of polypyrrole with sugarcane bagasse cellulosic biomass and adsorption efficiency for 2,4 dichlorophony acetic acid in column mode. *J Mater Res Technol* 2021;15:2016-25.
<https://doi.org/10.1016/j.jmart.2021.09.028>.
- [9] Jia Z, Li Z, Ni T, Li S. Adsorption of low cost absorption materials based on biomass (*Cortaderia selloana* flower spikes) for dye removal: kinetics, isotherms and thermodynamic studies. *J Mol Liq* 2017;229:285-92.
<https://doi.org/10.1016/j.molliq.2016.12.059>.
- [10] Maqbool M, Sadaf S, Bhatti HN, Rehmat S, Kausar A, Alissa SA, et al. Chemically modified sugarcane bagasse-based biocomposites for efficient removal of acid red 1 dye: kinetics, isotherms, thermodynamics, and desorption studies. *Chemosphere* 2022;291:132796.
<https://doi.org/10.1016/j.chemosphere.2021.132796>.
- [11] Yu J, Zhang X, Wang D, Li P. Adsorption of methyl orange dye onto biochar adsorbent prepared from chicken manure. *Water Sci Technol* 2018;77:1303-12.
<https://doi.org/10.2166/wst.2018.003>.
- [12] Hashem A, Badawy SM, Farag S, Mohamed LA, Fletcher AJ, Taha GM. Non-linear adsorption characteristics of modified pine wood sawdust optimized for adsorption of Cd(II) from aqueous systems. *J Environ Chem Eng* 2020;8:103966.
<https://doi.org/10.1016/j.jece.2020.103966>.
- [13] Yang S-S, Chen Y-d, Kan J-H, Xie T-R, He L, Xing D-F, et al. Generation of high-efficient biochar for dye adsorption using frass of yellow mealworms (larvae of *Tenebrio molitor* Linnaeus) fed with wheat straw for insect biomass production. *J Clean Prod* 2019;227:33-47.
<https://doi.org/10.1016/j.jclepro.2019.04.005>.
- [14] Ahmad A, Khan N, Giri BS, Chowdhary P, Chaturvedi P. Removal of methylene blue dye using rice husk, cow dung and sludge biochar: characterization, application, and kinetic studies. *Bioresour Technol* 2020;306:123202.
<https://doi.org/10.1016/j.biortech.2020.123202>.
- [15] K. Prabhakaran, T. Mohanapriya, M.G. Geena and E. Kavitha Development and Characterization of an Eco-friendly Stishovite Clay-manganese Dioxide Nanocomposite for Efficient Dye Removal from wastewater. *J. Environ. Nanotechnol.* Vol .13(4), 259-303 (2024).
<https://doi.org/10.13074/jent.2024.12.244979>.
- [16] Venkateswaran Vinayagam, Priya Thangaraju. Equilibrium and Kinetics of Adsorption of Cationic Dyes by Stishovite clay- TiO₂ Nanocomposite. *International Journal of Modern Engineering Research (IJMER)*, Vol.2, Issue.6, Nov-Dec. 2012 pp-3989-3995. www.ijmer.com